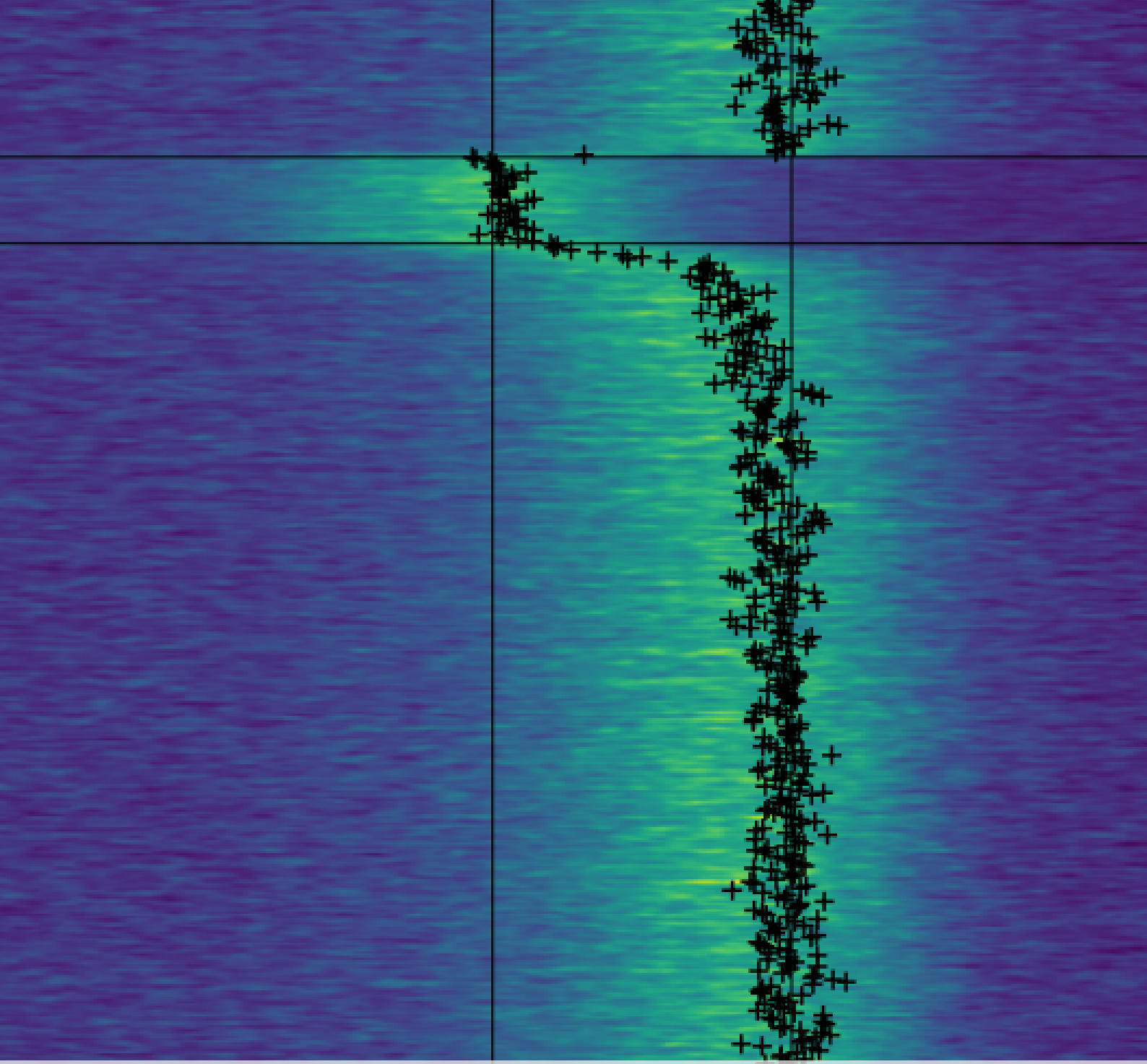

Effects of Carbon Functionalization on Hydrogen Oxidation Underneath Graphene Flakes

Author: Johannes Stubbe

Supervisor: Jan Knudsen
Co-Supervisor: Virginia Boix

Degree: B.Sc.
Project Duration: 3 month
Department: Physics
Division: Synchrotron Physics

Contents

Table of Acronyms

Acronym	Meaning
XPS	X-Ray Photoelectron Spectroscopy
APXPS	Ambient-Pressure X-Ray Photoelectron Spectroscopy
UHV	Ultra High Vacuum
CVD	Chemical Vapor Deposition
TPG	Temperature Programmed Growth
FWHM	Full Width at Half Maximum
HWHM	Half Width at Half Maximum
ML	Monolayer
MLE	Monolayer Equivalent

Abstract

Effects of carbon functionalization on the catalytic properties of the space underneath epitaxial graphene flakes on Ir(111) are investigated with Ambient Pressure X-ray Photoelectron Spectroscopy studies of oxygen hydrogenation. The 0.1 mbar oxygen atmosphere hosting O-intercalated graphene flakes was replaced with hydrogen pulses lasting 50 s each, triggering the water formation. Underneath pristine graphene flakes on a reference sample, a previously discovered [1], super-dense OH-H_2O phase was captured. The same OH-H_2O phase was observed underneath C-functionalized graphene flakes during the hydrogen pulses at 45°C but not at 75°C. This temperature dependence can be explained by the OH-H_2O phase being unstable underneath graphene and the water molecules gaining the mobility to escape in the temperature range between 45°C and 75°C. That leads to the conclusion that C-functionalization effectively changes the chemistry underneath graphene flakes and is a promising approach for the development of highly selective, graphene based catalysts.

1 Introduction

Graphene is an allotrope of carbon that corresponds to a single atomic layer of graphite. It has a two-dimensional honeycomb structure, which means that every C-atom binds to three neighboring C-atoms as depicted in figure 1. A carbon atom forming bonds with three neighbors is sp^2-hybridized, while a C-atom forming bonds with four neighbors, like in a diamond, are said to be sp^3-hybridized.

The first successful isolation of graphene was done by the scotch tape method in 2004 by Andre Geim and Konstantin Novoselov.[2] The term 'scotch-tape-method' describes the exfoliation of graphene from highly oriented graphite with scotch tape and subsequent dissolving of the adhesive, leaving one layer of C-atoms.

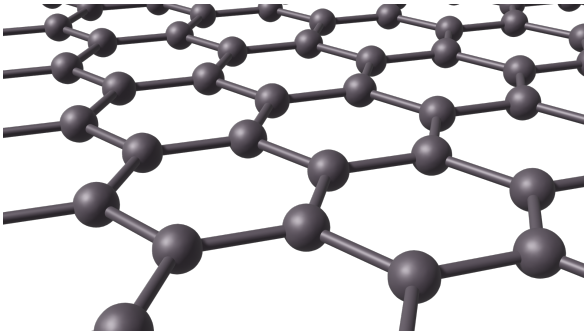

Figure 1: Hexagonal structure of graphene.

This discovery boosted the research in graphene and other 2D-materials and led to the development of other methods for producing graphene. A procedure that has proven to consistently produce graphene films of high quality is the thermal decomposition of hydrocarbons on the highly oriented surfaces of transition metals. An example of thermal decomposition is the dosing of ethylene (C_2H_4) onto a hot metal substrate. Upon adsorption, the ethylene molecules dissociate, and the hydrogen desorbs in the form of H_2 while the carbon atoms form graphene on the metal surface. This method of supporting the growing graphene on a crystalline structure is called epitaxial growth and allows to regulate the coverage of the sample. Therefore, it is possible to grow graphene flakes covering fractions of the substrate, instead of a film covering the entire substrate.
The most perfect graphene films have been observed on the hexagonal structure of an iridium Ir(111) surface, which is the substrate that I used for my experiments.[3]

Graphene grown on Ir(111) is loosely bound to the substrate and if the graphene film is defective and has holes, gaseous atoms from the outside can enter and move into the space between the graphene and the substrate. This process is called intercalation and has been observed and studied for many different gases. If, for example, O_2 or H_2[4, 5] are dosed, the molecules dissociate on the Ir substrate, move underneath the graphene and lift it up.[6, 7] This process is illustrated in figure 2. Entire molecules such as CO have also been intercalated underneath graphene.[8]

Studying the intercalation of graphene on a substrate is a way to investigate the interaction of sp^2-hybridized carbon with atoms in the confined space below them. That knowledge can then be transferred to other structures involving highly oriented sp^2-hybridized carbon, that are more difficult to study due to their geometry, such as nanotubes or fullerene balls.

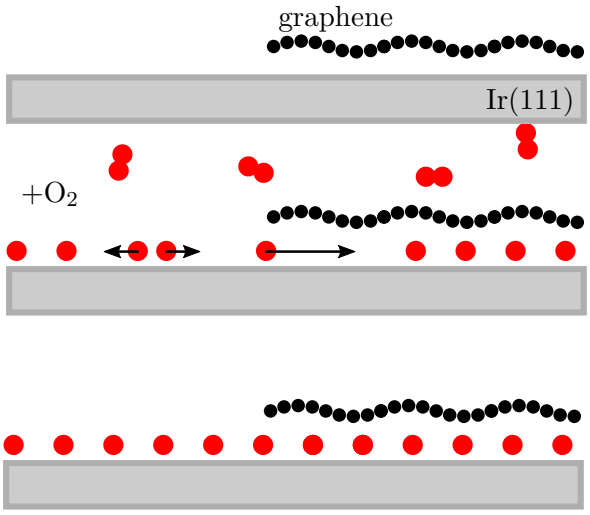

Figure 2: Illustration of O-intercalation between graphene and iridium.

Studies that exposed CO-intercalated graphene flakes to O_2 afterwards found CO_2 underneath the flakes.[9, 10] This observation reveals that oxidation and hence chemical reactions can happen in the confined space between graphene and the Ir substrate. More striking was the investigation of water formation underneath graphene flakes covering half of an Ir(111) substrate.[1, 11] In those experiments, O-intercalated graphene flakes were exposed to H_2 and afterwards studied under UHV conditions. Instead of only H_2O, a dense OH-H_2O phase was observed underneath the graphene. This OH-H_2O phase was only observed in the confined space underneath graphene flakes and indicates fascinating catalytic effects imposed by this restriction.

Not only the space below graphene can be intercalated, the top of the graphene can be altered by selectively adding atoms. This process is called functionalization and has been studied for different elements. Functionalization of graphene is usually done by exposing the film to radicals because their high reactivity allows them to adsorb on top of the layer. This process has been studied, noticeably by exposure of graphene to atomic H-, O- and C-atoms.

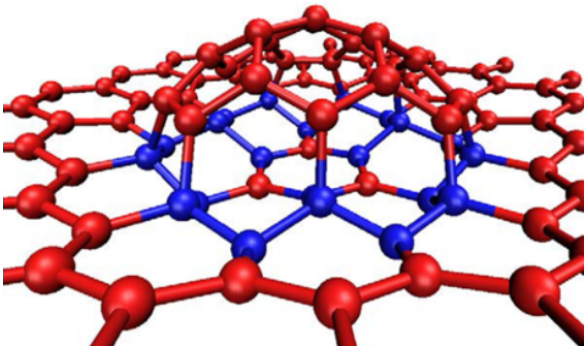

Figure 3: Carbon-clusters form on graphene upon C-exposure. Reproduced from [12].

In case of H- and O-functionalization, the adsorbed atoms arrange into periodic patterns on the graphene surface and bind directly to some of the C-atoms in the graphene.[13] These bonds from above induce neighboring C-atoms to bind downwards to the Ir(111) substrate which effectively pins the entire graphene film down.[14, 13]

Whilst for H-and O-functionalization, every atom of the adsorbate binds directly to the graphene, domelike C-clusters form if graphene is treated with atomic carbon, as illustrated in figure 3. Those structures are again periodically distributed, and pin the graphene film down to the substrate in a similar manner as the H or O. These C-clusters possess an extraordinarily high thermal stability and have been shown to withstand temperatures of 1000°C, whilst the H and O was etched from the graphene surface at 700 and 500°C, respectively.[14, 15, 12]

While both, intercalation and functionalization, have been extensively studied as separate processes, surprisingly few studies have been published about intercalation under functionalized graphene.

Recent Ambient Pressure X-ray Photoelectron Spectroscopy (APXPS)[1] studies investigated water formation underneath pristine graphene flakes. The water formation was induced by exposing O-intercalated graphene flakes to pulses of H_2 gas. A great advancement over earlier studies was using an ambient pressure setup allowing to monitor the reaction in a near realistic pressure environment. My work continues those studies by investigating the effects of C-functionalization on water formation under graphene. Two series of APXPS measurements were undertaken. First, a sample with unfunctionalized O-intercalated graphene flakes was exposed to pulses of H_2 while its binding energies were being probed. Then the measurements were repeated after functionalizing the graphene flakes with C-clusters.

The first part of the method section of this thesis deals with data acquisition with an APXPS setup and subsequent data treatment. Then specifics of epitaxial graphene growth on Ir(111) are discussed.

In the result section, the C-functionalized graphene flakes are characterized and compared to publications. After that, a comparison of O-intercalation under graphene flakes with and without C-clusters is conducted. The same will be done for the water formation experiments which were undertaken at two different temperatures, first at 75°C and later at 45°C to probe kinetic effects. The thesis will close with a summary of the conclusions and an outlook suggesting follow-up experiments.

[1] APXPS is an experimental technique that can determine the binding energy of core electrons of different elements at pressures in the mbar regime and hence can be used to probe samples while exposing them to gases.

2 Method

2.1 X-Ray Photoelectron Spectroscopy

The experimental technique used for this thesis work was X-Ray Photoelectron Spectroscopy (XPS). It uses the photons of monochromatic x-rays to induce photoemission of core level electrons as depicted in figure 4. From the known photon energy and the measured kinetic energy, the binding energy of the core level can be calculated. Since the binding energies of core levels are distinct for different elements, they can be used to determine the elemental composition of a sample. The binding energy E_B can be defined as the difference between the energies of the atom before E_i and after E_f removal of the electron. That means, the binding energy of an electron at the Fermi level must be 0 eV. When an atom is hit by a photon of energy $h\nu$ greater than the sum of binding energy and work function of the sample ϕ_{sample}, an electron will be excited and leave the atom with kinetic energy E_K. The relation between binding energy, kinetic energy and photon energy is illustrated in figure 5.

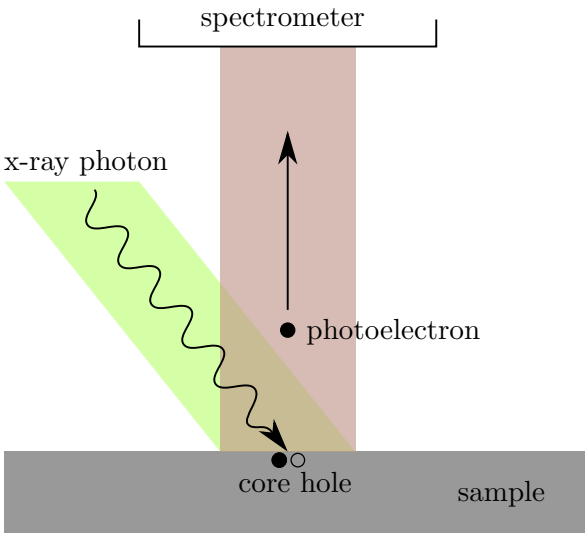

Figure 4: Schematic of the photoemission process during XPS. A photon from a monochromatic beam of x-rays excites a core-level electron in a sample which travels toward the spectrometer leaving a core hole behind.

$$E_B = E_i - E_f = h\nu - E_K - \phi_{sample} \quad (1)$$

The first part of equation 1 nicely highlights that the binding energy is dependent on both, the initial and the final state of the atom. Initial state effects caused by changes of the local potential are of particular importance in this thesis. Oxidation of an atom, for example, will pull the valence electron density further from its core, which will turn that atom more electropositive and make the core level electrons more

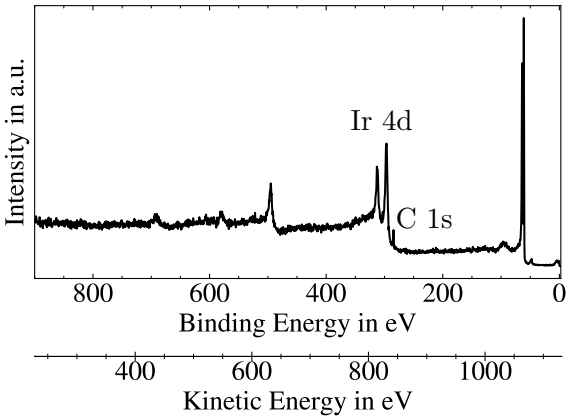

Figure 5: XP-Spectrum of graphene on Ir(111) at a photon energy $h\nu = 1150$ eV with Kinetic Energy and Binding Energy scaling.

tightly bound.

Figure 6 depicts the XP-spectrum of the C 1s region of an Ir(111) sample with graphene after exposure to CO. Three peaks can be observed. The peak, labelled C_{CO}, is caused by the photoelectrons emitted from the carbon atoms in adsorbed CO molecules and is visible at 286.9 eV, the peak C_{Gu} at 284.1 eV originates from the atoms in the graphene and the peak C_{Gi} at 283.5 eV is caused by atoms from graphene that is CO intercalated.

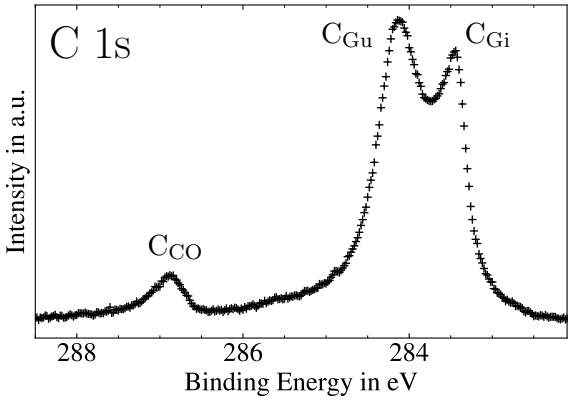

Figure 6: XP-Spectrum of the C 1s region of graphene after exposure to CO.

These differences of binding energy due to the presence of neighboring atoms are called chemical shift and can be used to determine the chemical environment of an atom.

Although the x-rays penetrate several micrometers of the sample and photoelectrons from many atomic layers are emitted, only a fraction of those electrons manage to leave the sample without losing energy.

The inelastic mean free path determines the distance λ, a beam of electrons with energy E can travel in a solid before its intensity has decreased by $1/e$. Typical kinetic energies of electrons in XPS range between 10 eV and 1000 eV resulting in an inelastic mean free path of a few Ångström, as shown in figure 7, and only the topmost atomic layers of the crystal are probed. Hence, XPS is very surface sensitive and a popular technique for the study of 2D-materials. Many electrons from deeper atomic layers arrive at the detector with decreased kinetic energies from scattering processes, though. That leads to the linear, step-like background observed in figure 5.

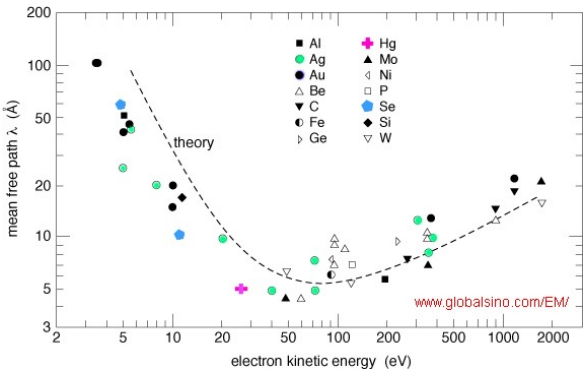

Figure 7: Inelastic mean free path of electrons in a solid. Reproduced from globalsino.com/EM

Electrons do not only have a short mean free path within solids, but in gases as well. The mean free path of an electron with 100 eV in 1 mbar of gas is at the order of 1 mm. Electron analyzers are large-scale instruments on the other hand and require the electrons to travel over a meter before reaching the detector. For this reason and in order to prevent atmospheric contamination of the samples, XPS experiments are usually performed

at ultra-high vacuum (UHV). Since real surface processes often depend on a gaseous atmosphere, that is a main limitation of conventional XPS. Ambient pressure XPS (APXPS) allows measurements in the mbar regime by introducing a differential pumping system. Figure 8 shows the schematics of the HIPP3 APXPS electron analyzer that I used for my experiments performed at the HIPPIE beamline at MAX IV.. The electrons enter a first pumping stage through a nozzle, 0.3 mm in diameter, placed 0.6 mm from the sample and continue towards the hemispherical analyzer, passing two more pumping stages with electrostatic lenses focusing the electron beam. A hemispherical electron analyzer consists of an inner, positively charged and an outer, negatively charged half sphere. This setup bends the path of the electrons proportional to the square of their speed v^2 and hence can discriminate between different kinetic energies.

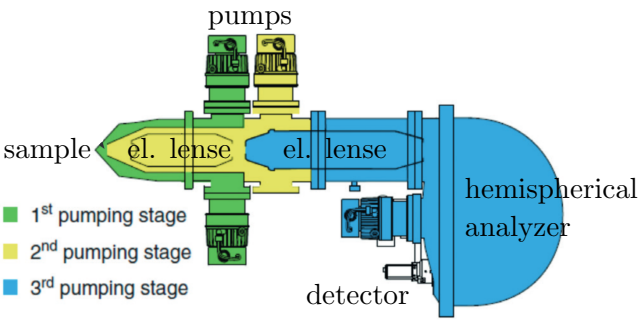

Figure 8: Schematics of a HIPP3 electron analyzer. Modified from scientaomicron.com.

The detector consists of three parts. At a first stage, the electrons pass through a microchannel plate, which can be visualized as a plate consisting of many small electron multipliers. Hence, out comes an electron shower which in a second step hits a fluorescent screen, that is filmed with a digital camera.

2.2 Spectra Treatment and Curve Fitting

In order to correct for changing photon energies, the Fermi edge (FE) was calibrated for every spectrum (figure 9).

Literature articles are dominated by two different kinds of background removal, linear background removal and polynomial removal (figure 10). Since this work is heavily comparing newly obtained spectra with earlier discoveries, both kinds of background treatment were used.

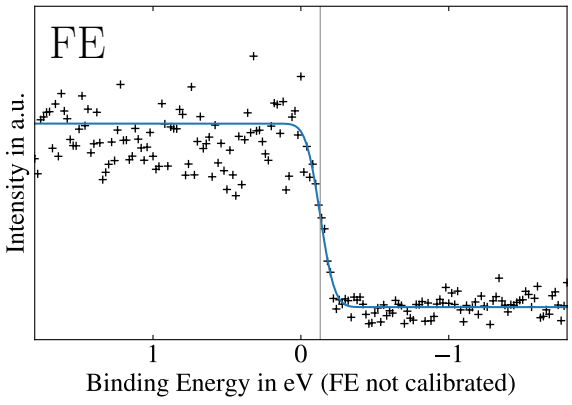

Figure 9: Fermi edge calibration: The offset between the horizontal line and 0 eV can be corrected.

The peak shapes in XP-spectra are subject to two major broadening effects. Natural broadening is caused by the limited lifetime of the core hole left after exciting the electron. This lifetime is defined through Heisenbergs uncertainty principle $\Delta E \cdot \Delta t \geq \hbar/2$

and gives rise to a Lorentzian peak shape

$$L(E;\gamma) = \frac{1}{\pi\gamma}\frac{\gamma^2}{E^2+\gamma^2}$$

where E represents the Energy and γ is the half width at half maximum (HWHM)
Additionally, experimental broadening, which is related to the energy resolution of the

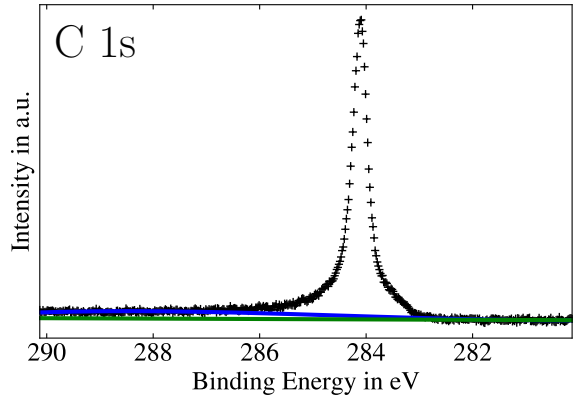

Figure 10: Comparison of a polynomial (blue) and linear (green) background.

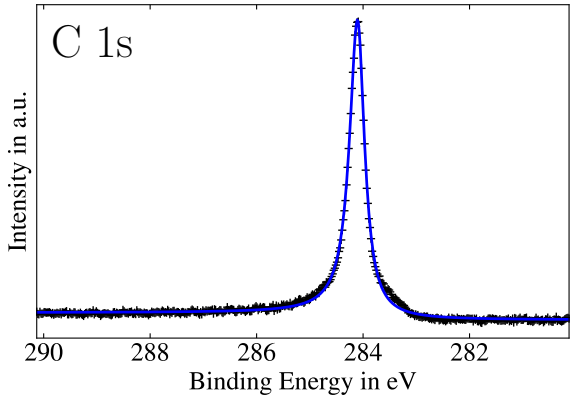

Figure 11: XPS peak fitted with an asymmetric Voigt profile (blue line).

detector and the photons, causes a Gaussian peak shape with HWHM σ

$$G(E;\sigma) = \frac{1}{\sigma\sqrt{2\pi}}e^{-\frac{1}{2}\left(\frac{E}{\sigma}\right)^2}.$$

A Voigt profile is the convolution of a Lorentzian and a Gaussian function and can be used to represent the line shape of an XPS peak. There is no analytical expression for the Voigt shape, but it can be related to the Faddeeva-function w for which good approximations exist.

$$V(E;\gamma,\sigma) = \int_{-\infty}^{\infty} G(E';\sigma)L(E-E';\gamma)dE' = \frac{\mathrm{Re}(w(z))}{\sigma\sqrt{2\pi}} \quad | \quad z = \frac{E+i\gamma}{\sigma\sqrt{2}}$$

Especially in metals, the big number of electrons in the valence band close to the Fermi edge lead to excitation of electron-hole pairs by the passing photoelectron. Hence, XPS peak shapes are often observed to be asymmetric and a simple Voigt profile is not enough. As a correction, so-called asymmetric Voigt profiles, consisting of two Voigt profiles linked in the peak, can be used to approximate the peak shape.

2.3 Graphene Growth on Ir(111)

The transition metal Iridium (Ir) served as the substrate, upon which the graphene was grown. Ir has a face centered cubic (fcc) crystal structure and its (111) surface has a hexagonal structure with an in-plane lattice constant of 2.72 Å.[3]

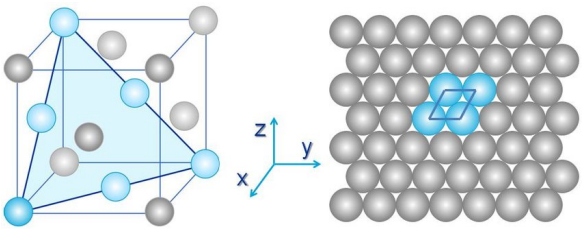

Figure 12: (a) Unit cell of a fcc crystal. (b) Atomic surface layer of the (111) plane of a fcc crystal. Reproduced from [16].

On highly oriented transition metals, graphene can be grown epitaxially by thermal decomposition of ethylene. In order to achieve full graphene coverage, 1.0 monolayers[2] (ML), a method called Chemical Vapor Deposition (CVD) is used. Using the CVD method to grow graphene on Ir(111), the crystal is heated to 900°C and exposed to C_2H_4 vapor at 10^{-7} mbar for at least 30 minutes. The ethylene dissociates instantly upon contact with the bare iridium surface and carbon atoms adsorb on the surface forming graphene while the hydrogen atoms leave as H_2. Ethylene molecules do not react with the graphene film and hence the process is self-limited to one layer of atoms.[18, 3]

Graphene has a lattice constant of 2.46 Å[19], which is smaller than the 2.72 Å in-plane lattice constant of Ir(111). This lattice mismatch results in a so-called moiré pattern where 10 graphene unit cells (2 atoms each) match 9 surface unit cells (1 atom each) of the Ir substrate as illustrated in figure 13.

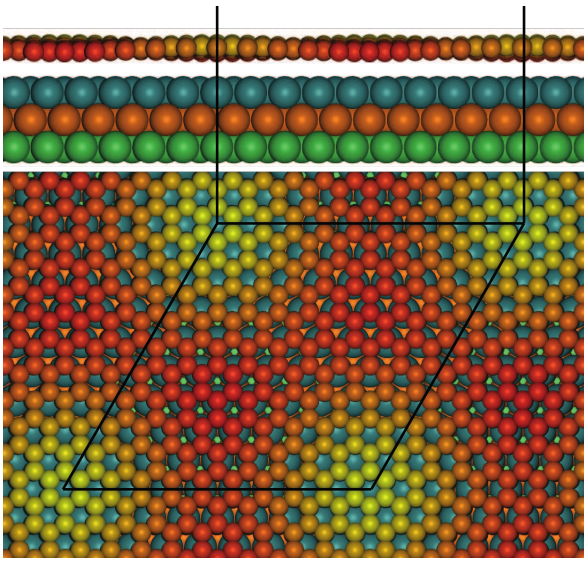

Figure 13: Visualization of a graphene film on Ir(111). The lattice mismatch causes a moiré pattern. Reproduced with permission of Jan Knudsen.

The graphene is bound weakly to the substrate by van der Waals forces, but still differences in attraction to the Ir(111) are seen depending on the overlay of the C-atoms with the substate. That gives rise to the wavelike hight-pattern of the graphene, that is indicated by the color code in figure 13.

To achieve graphene coverages of less than 1.0 ML, a variation of CVD is utilized. Temperature Programmed Growth (TPG) consists of ethylene exposure at room temperature

[2] 1.0 ML graphene is equivalent to a density of 3.8×10^{19} atoms/m^2 [17]

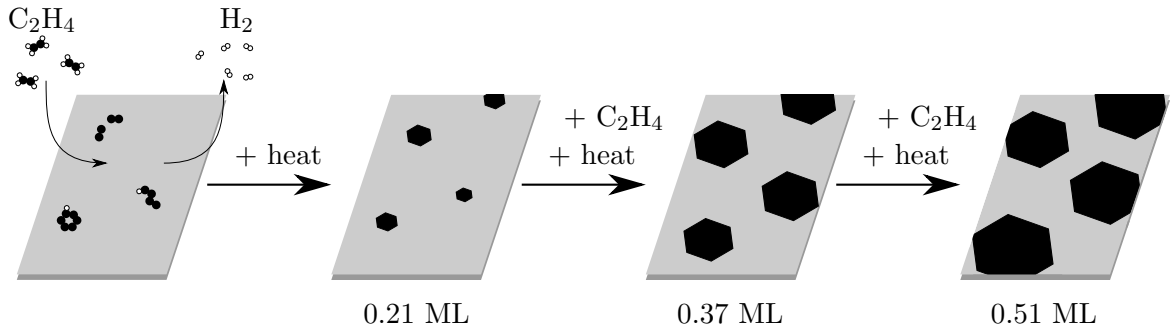

Figure 14: Illustration of TPG growth of 0.51 ML graphene.

and subsequent annealing of the sample at high temperature in vacuum. At room temperature, the ethylene only dissociates partly on the iridium surface and form an amorphous structure. When the sample is heated afterwards, the carbon structure dissociates as during CVD and graphene is formed. Since graphene is more dense than the amorphous structure, the coverage after one TPG cycle is 0.21 ML of the bare Ir(111) surface.[18] Repeating this process three times will result in a graphene coverage of

$$1 \cdot 0.21 \text{ ML} + (1 - 0.21) \cdot 0.21 \text{ ML} + (1 - 0.21 - (1 - 0.21) \cdot 0.21) \cdot 0.21 \text{ ML} = 0.51 \text{ ML}.$$

3 Results

3.1 C-Functionalization of Graphene

Since this work aims to determine how carbon clusters atop graphene affect the chemistry below, specific focus should be laid on the carbon cluster functionalization of graphene. We were aiming to reproduce carbon structures on top of graphene as described by Herbig et al [12]. The clusters in that paper were grown by exposing 1 ML of graphene to carbon vapor, while we wanted to produce clusters on top of 0.5 ML graphene flakes. Carbon vapor was created by sublimation from a solid carbon rod in a commercial E-beam evaporator. A quartz balance was used to estimate the deposition rate and it was found, that with a voltage of 1000 V and an emission current of 110 mA, 30 minutes were needed to obtain an approximate coverage of 0.3 monolayer equivalents (MLE), which relates the number of C-atoms to monolayers of graphene. Those settings were applied when functionalizing the graphene flakes.

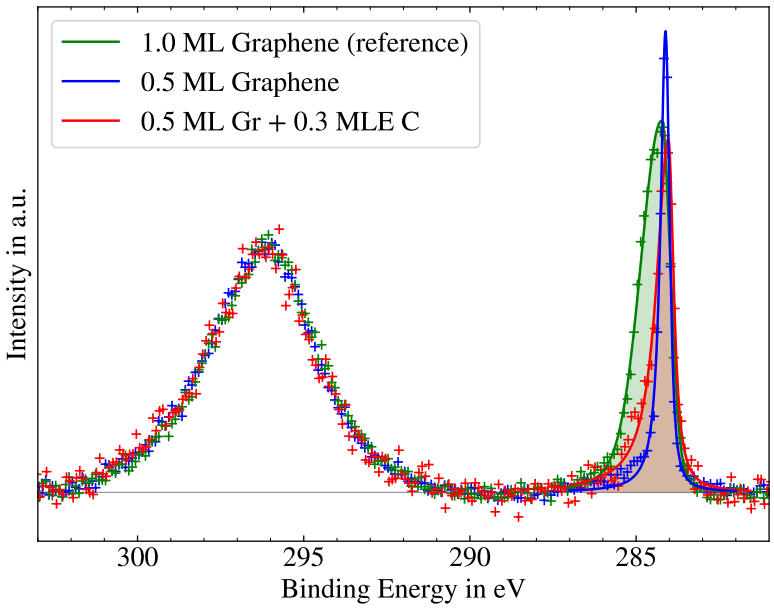

Figure 15: Coverage calibration of graphene.

In order to determine the cluster coverage precisely, figure 15 displays three XP-spectra of the Ir 4d – C 1s region. The blue crosses mark the spectrum of 0.5 ML graphene grown with three CVD-flashing-cycles as explained earlier. The red spectrum was taken after 30 min of C-functionalization of the 0.5 ML graphene sample, while the green crosses represent a spectrum of graphene grown according to the recipe for 1.0 ML graphene. The spectra are scaled to the integral over their Ir $4d_{5/2}$ peak at 296 eV and asymmetric Voigt profiles, represented by the solid lines, are fitted to the individual C 1s peaks.
Since the spectra were scaled to a peak of the iridium substrate and the number of C 1s photoelectrons must be proportional to the number of carbon atoms on the sample, the carbon coverage of a sample can be approximated by comparing the areas underneath the C 1s peaks. Taking the green area corresponding to 1.0 ML as a reference, the coverage of the blue and red spectrum can be calculated to 0.48 ML and 0.70 MLE, respectively.

Because the recipes for CVD growth of graphene have proven to be very consistent in the deposited amount of carbon, the method for coverage calibration can be evaluated by comparing the relative coverages the two samples with 1.0 ML and 0.5 ML coverage. A value of 0.48 matches well the expected coverage after 3 TPG-cycles [18] and thereby validates the coverage calibration method.

The amount of deposited carbon when growing the clusters was determined to correspond to 0.70 MLE. That means, that 0.70 MLE − 0.48 MLE = 0.22 MLE instead of 0.3 MLE of carbon atoms were added to the graphene. Since the quartz balance used to estimate the amount of carbon deposition earlier, is a crude and rather imprecise tool, large variations are not surprising.

The fraction of the 0.22 MLE that adsorbs on the graphene flakes must be equal to $0.48 \cdot 0.22$ MLE = 0.11 MLE on the graphene flakes. Assuming that one C-cluster adsorbs in each moiré unit cell[12] and knowing that each moiré cell contains 200 atoms gives an average cluster size of $0.11 \cdot 200$ atoms = 21 atoms.

Having determined the coverage of the carbon clusters, we continue with the spectral C 1s fingerprints and compare this to the published spectra from the literature. Figure 16 compares spectra of the C 1s peak of 0.5 ML graphene before (lower panel) and after deposition of 0.22 MLE carbon (upper panel). The black crosses mark datapoints from the measurement and the solid red lines represent curve-fits with the colored components below. As shown in earlier experiments [3, 20] the C 1s peak of the pristine graphene can be represented by a single asymmetric Voigt profile at 284.10 eV with a FWHM of 0.34 eV.

The functionalized sample can be fitted with three additional components. The main component C_{Ir} broadened by 1.1 eV to a FWHM of 0.55 eV. The three additional components are fitted with a symmetric Voigt profile with the same FWHM.

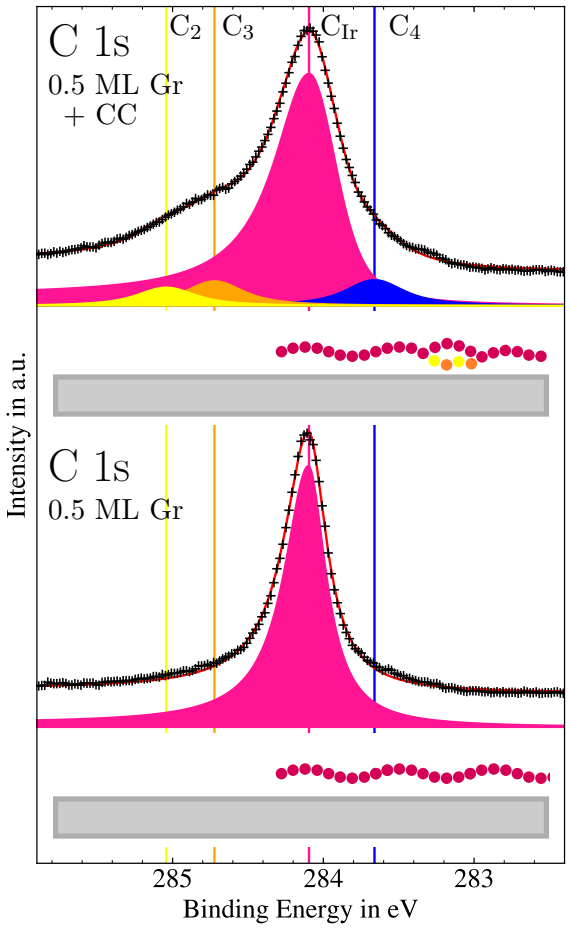

Figure 16: XPS spectra of the C 1s region before (bottom) and after C-functionalization (top).

They are located at C_2=285.03 eV, C_3=284.74 eV and C_4=283.68 eV. A similar peak shape was observed by Herbig et al. In their work, the C 1s component after cluster growth of 0.3 MLE on 1.0 ML graphene was fitted with 4 components located at C_{Ir}=284.04 eV (-0.05 eV), C_2=284.92 (-0.11 eV), C_3=284.54 eV (-0.20 eV) and C_4=283.48 eV (-0.20 eV). The differences between the measurements during this beamtime and the published work can be attributed to variations in the chemical environment of both systems, most importantly the original system in the reference experiment being entirely covered by a full monolayer of graphene whilst my experiment used graphene flakes covering 50 % of the iridium. Hence, additionally to the reactions on top of the graphene flakes, the atomic carbon vapor can attach to the bare iridium patches and form amorphous carbon structures.

Figure 17 is a visualization of a DFT optimized model of a single carbon cluster formed on graphene after exposure to carbon vapor. The red and blue atoms are sp^2- and sp^3-hybridized, respectively, while the iridium substrate is omitted for better visibility. This model system consists of one moiré unit cell of pristine graphene with 19 additional C-atoms corresponding to 0.1 MLE. It is notable, that according to this simulation, the 19 newly deposited C-atoms rearrange to form a domelike shape which makes 21 atoms in the original graphene layer switch from sp^2- to sp^3-hybridization. However, variations in size of the clusters are possible. This figure is helpful interpreting the additional peaks found in figure 3.

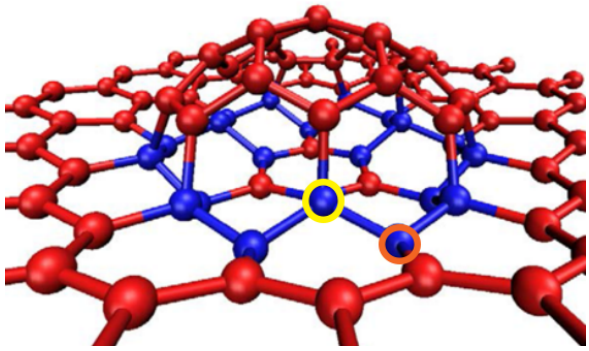

Figure 17: DFT model of a C-cluster. Reproduced from [12]

Since the range from 284.9 eV to 285.2 eV is associated to the sp^3-hybridized atoms in diamond-like structures, the two components, C_2 and C_3, which are forming the high energy shoulder of the peak can be linked to newly sp^3-hybridized atoms in the original graphene layer. In figure 17, two different kinds of sp^3-hybridization can be observed. Firstly, the atoms that are binding upwards (yellow circle), directly to the additional carbon atoms forming the cluster. Secondly, the atoms (orange circle) in the graphene layer that are neighboring two upward binding get sp^3-hybridized downward and bind to the iridium substrate. In experiments with Pt-clusters on graphene, both effects causing sp^3-hybridization, have been observed to cause shoulders on the high energy side of the C 1s peak, that are similar in shape to the shoulder consisting of the components at C_2 and C_3. [20, 21]

Herbig et al argued that the peak at C_4=283.68 is caused by individual C-atoms that

have penetrated the graphene film and adsorbed on the iridium below. That explanation is consistent with our results, since the C_4 peak intensity of our sample where half of the iridium surface is unprotected has increased compared to the peak intensity of the fully covered sample in the article.

The article states "variations in the chemical environment and doping of the sp^2-hybridized graphene atoms" as reason for the broadening and slight shift of the C_{Ir}-peak. I would however like to make a more detailed connection to figure 17. The binding energy of 284.09 eV is specific to the sp^2-hybridized atoms in graphene. For pristine graphene, this peak is very defined and sharp because in graphene without defects, every carbon atom is equivalent and hence has the exact same binding energy. After C-functionalization some of the sp^2-hybridized form bonds to sp^3-hybridized graphene, which is chemically different and hence the binding energy of the sp^2-hybridized atom changes a little and the entire peak broadens. Furthermore, the added C-atoms are forming a fullerene-like dome of sp^2-hybridized atoms. A tempting explanation is that due to this spherical geometry, the bonds are angled differently, shifting the binding energies of the affected atoms.

3.2 Oxygen intercalation underneath graphene

In order to probe water formation underneath the graphene flakes, they first had to be intercalated by oxygen. In my experiments, this was done by dosing O_2 at 0.1 mbar with a flow of 1.2 standard cubic centimeters per minute (sccm) while heating the sample from room temperature to 75°C using a heating rate of 10°C/min. This procedure was applied to both, graphene flakes with and without carbon clusters and the C 1s peak was followed in real time. The resulting spectra are not published. For both samples, a C 1s peak shift towards lower binding energy could be observed. In case of the unfunctionalized graphene, the peak starts shifting at about 50°C and stops approximately 2:30 minutes later when the temperature reaches 75°C. The C 1s peak shift of the sample with carbon clusters starts at a similar temperature but took much more time and stopped more than 10 minutes after the temperature of 75°C was reached.

Figure 18 depicts C 1s XP-spectra of graphene before (bottom) and after (top) exposure to 0.1 mbar oxygen. The spectra in panel (a) were acquired on graphene flakes without carbon clusters atop and in panel (b) were acquired on the functionalized graphene flakes with the carbon clusters. The spectra before the oxygen exposure on the bottom have been extensively discussed in the previous section.

Comparing the upper spectrum of panel (a) with the lower spectrum, one major difference can be observed. The position of the C 1s peak has shifted by -0.53 eV from 284.09 eV before to 283.56 eV after oxygen exposure. Grånäs et al. studied the temperature

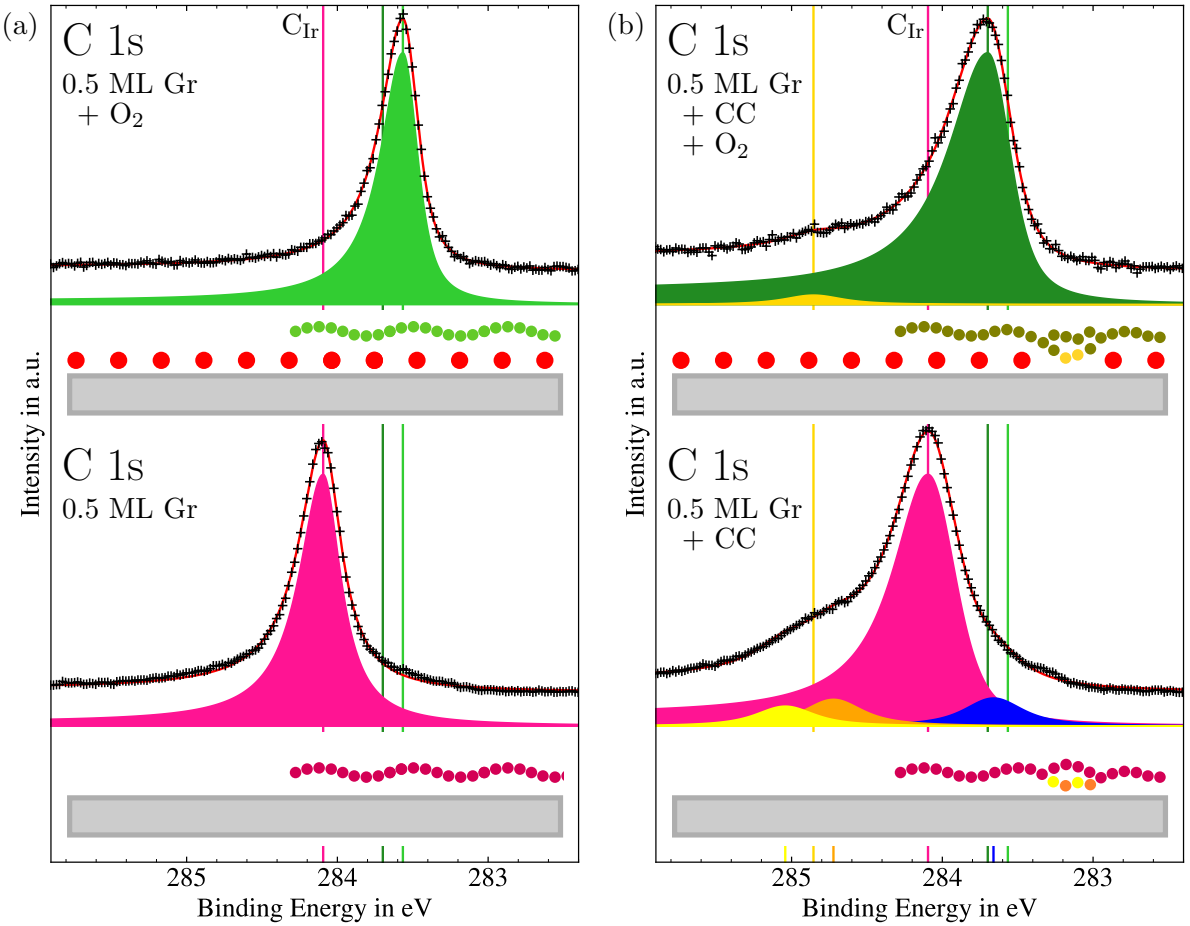

Figure 18: (a) XP-spectra of 0.5 ML pristine graphene before (bottom) and after (top) exposure to O_2. (b) XP-spectra of 0.5 ML C-functionalized graphene before (bottom) and after (top) exposure to O_2.

dependence of that process on a system similar to ours with 0.5 ML graphene on an Ir (111) substrate, but at a pressure of 10^{-5} mbar instead of 0.1 mbar in our experiment.[7] Contrary to our results, that publication found a C 1s peak position of 284.03± 0.02 eV at 75°C and full intercalation at 130°C indicated by a peak position of 283.64 ± 0.02 eV, corresponding to a shift of -0.45 ± 0.02 eV. These discrepancies can be attributed to the different pressures. The relatively high pressure in our experiment probably helped to push the oxygen under the graphene flakes. That would lead to a lower temperature needed for full intercalation and a higher density of oxygen underneath the graphene flakes which is indicated by the larger shift of the C 1s peak. The process of O-intercalation between Ir and graphene was described by Grånäs et al. [7, 1]: O_2 adsorbs dissociatively and forms a p(2×1) structure on bare iridium. When the Ir surface is completely oxidized, the O-atoms diffuse underneath the graphene and keep binding down to the iridium substrate while the graphene remains sp^2-hybridized and gets lifted up without binding to

the O below or the O_2 above.[7, 22] This lifting-up process decouples the graphene from the Iridium which dopes (moves the charge density towards) the graphene. That results in the shift of the C 1s peak towards lower binding energy.

The C 1s spectrum in panel b, with the carbon clusters, that was earlier fitted with four components can after exposure to O_2 be described with two components at 283.69 eV and 284.85 eV, respectively. The shift of the main peak corresponds to -0.40 eV and can again be attributed to O-intercalation. However, the peak position coincides with the peak position of the blue peak, that represents C-monomers, not belonging to the graphene flakes. The peak has a high gaussian contribution to the Voigt profile on the high energy side, which makes it lean to the right. That can be explained with the carbon clusters on top of the flakes binding them to the substrate which makes it harder for the atomic oxygen to diffuse under the flakes and perhaps prevents that entirely, directly underneath the clusters. The high energy shoulder indicating the sp^3-hybridized atoms, that are responsible for the pinning down of the flakes was described by two components at 285.03 eV and 284.74 eV which can be attributed to 0.1 MLE before O_2 exposure. In the oxygen atmosphere, the shoulder loses definition and intensity. It can be fitted with one component at 284.85 eV between the original positions and the intensity corresponds to 0.04 MLE of carbon atoms. That indicates that on average, only 8 atoms per graphene unit cell remain sp^3-hybridized and most of the atoms forming four bonds switched back to sp^2-hybridization due to the uplifting effects of the O-intercalation.

3.3 Hydrogen Pulsing

In figure 19 we compare C 1s image plots of 0.5 ML pristine graphene (left) and 0.5 ML graphene with C-clusters atop (right). These spectra were acquired in snapshot mode with a frequency of 1.42 Hz over a period of 1300 s. Both measurements were recorded while the sample was exposed to a flow of 10 sccm of O_2 at a pressure of 1 mbar and 75°C. The black crosses mark the C 1s peak positions determined for simplicity by curve fitting of the individual spectra with a single asymmetric Voigt profile. The vertical line at 284.09 eV indicates the peak position of unintercalated graphene on iridium.
In both cases the graphene is O-intercalated from the start, visible by the C 1s peak position of 283.6 eV. Four pulses of hydrogen were dosed for 50 s each and separated by pure oxygen flow for 300 s. Each H_2-pulse was formed by lowering the O_2 flow to 1 sccm while mixing with 9 sccm H_2 at the same time. In panel a, without carbon clusters, we see that upon arrival of the hydrogen pulses, the C 1s peak shifts from its O-intercalated position at 283.59 eV to 284.30 eV. As no crosses are observed between the two peak

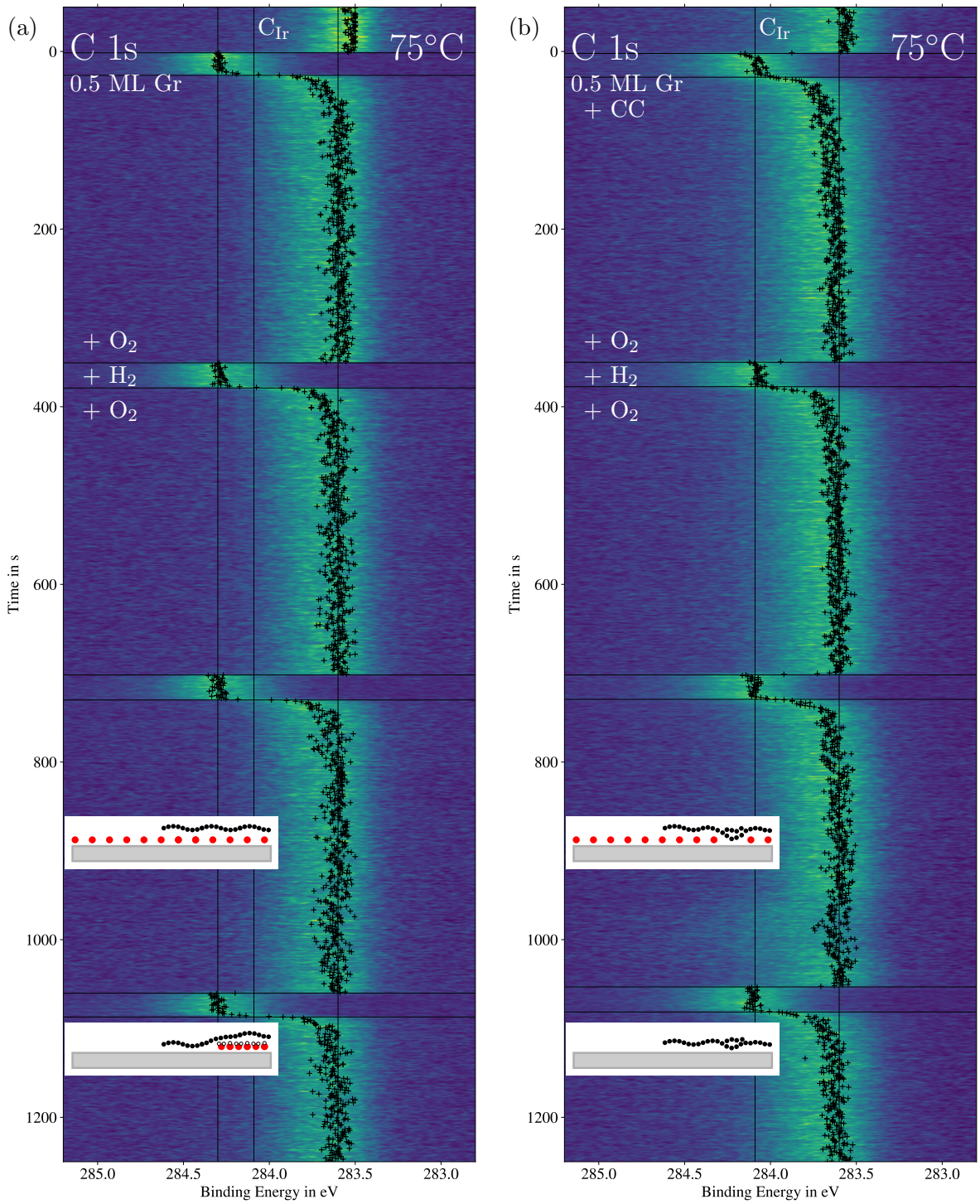

Figure 19: (a) XP-spectra of 0.5 ML pristine graphene before (bottom) and after (top) exposure to O_2. (b) XP-spectra of 0.5 ML C-functionalized graphene before (bottom) and after (top) exposure to O_2.

positions upon arrival of the H_2 pulses, we conclude that the peak shift happens very fast and the duration of the shifting cannot be resolved with a time resolution of 1.42 Hz. The shifted binding energy of 284.30 eV corresponds to a difference of +0.22 eV compared

to the position of pristine graphene at 284.09 eV and it indicates the intercalation of an OH-H_2O phase below graphene according to the work of Grånäs et al. [1]

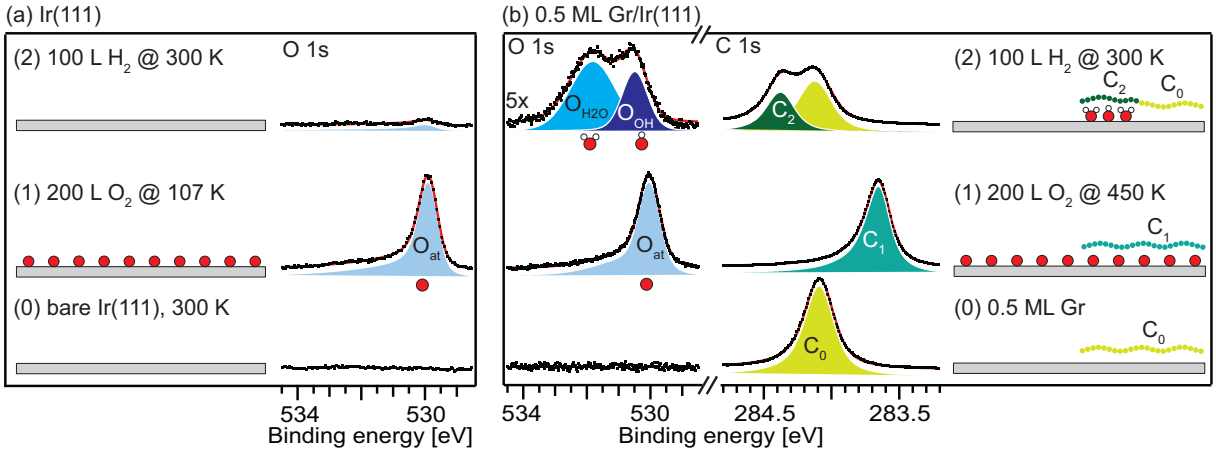

Figure 20: Comparison of room temperature H_2 exposure of an oxygen saturated Ir(111) surface without (left) and with (right) a cover of 0.5 ML Gr. Opposite to my work, these measurements were taken at UHV. Reproduced from [1]

In panel (a) of figure 20 which is reproduced from [1] without Gr, upon exposure to H_2, water is formed on the Ir surface and the H_2O molecules desorb, and the O 1s signal therefore disappears upon exposure to 100 L[3] H_2 at 300 K.
Figure 20 (b) shows how that process is different when the iridium is partly covered with Gr. Oxygen exposure leads to oxidization and O-intercalation underneath the graphene as described in the previous section. From previous studies it is known that the H_2 does not adsorb on a 1 ML graphene film that covers the entire Ir(111) surface [4]. However, when bare Ir patches exist, the H adsorbs dissociatively on the Ir patches not covered by graphene. Subsequently, the small hydrogen atoms can easily diffuse in under the graphene flakes where OH and H_2O is formed through the reaction with the oxygen underneath the graphene and those molecules become trapped.
The OH-H_2O phase is almost twice as dense as the intercalated oxygen, leading to parts of the flakes trapping the water phase whilst about half of the area of the graphene is not intercalated. Those two components can be distinguished by the C_2 peak at 284.37 eV and the pristine graphene peak at 284.09 eV in figure 20 (b) (2). In our measurements, only one peak at 284.30 eV can be observed, most likely because the resolution in snapshot mode is insufficient. Furthermore, it must be noted that the spectra in figure 20 were taken in UHV, after exposure to the gases. The spectra in figure 19, however represent the live measurements of the reaction during exposure to O_2 and H_2 at a pressure of

[3]Langmuir (L) is a surface-exposure unit. $1\text{L} = 1\ \text{torr} \cdot \mu\text{s} \approx 1.33\ \text{mbar} \cdot \mu\text{s}$

0.1 mbar. Hence, it cannot be excluded that the parts of the graphene flakes that are not intercalated by the OH-H_2O phase, are H-intercalated while in the H_2 atmosphere. H-intercalation would be indicated by a -0.15 eV shift of the binding energy compared to pristine graphene. [4] A shoulder at that position which might not be resolved in snapshot mode. The residence time of hydrogen underneath graphene at temperatures over 150 K is of the order of 1 ms. The peak remains at 284.30 eV for 27±1 s during every pulse and subsequently changes back to 284.59 eV signaling O-intercalation again. This shift from high to lower binding energy has a tail and hence is significantly slower than the shift in the other direction at the beginning of the pulse. This suggests that the in-diffusion of hydrogen under the graphene flakes and the subsequent OH and H_2O formation is a fast process, while the OH and H_2O out-diffusion and substitution by in-diffusion of O-atoms is a significantly slower process.
A possible reason for that is that OH and H_2O molecules are rather big molecules and quite restricted by the graphene when moving out while the small H-atoms can easily move in. A similar argument can be made for the oxygen that is moving in and bigger than the hydrogen, as well.

Comparing panel (a) and (b) of figure 19 without and with clusters, respectively, we observe that the image plots have similarities. Both peaks start at oxygen intercalated position, shift very fast to higher binding energy during the pulses while a tail is observed when shifting back to their original position. Upon arrival of the pulses, the peak in panel (b) shifts to 284.09 eV which is an indicator for unintercalated graphene on iridium. That implies that almost all the intercalated oxygen has left from underneath the graphene and no OH-H_2O phase has been captured.
This dramatic difference can be explained in two different ways. Either, the formation of OH and H_2O is completely prevented by the presence of the clusters and the intercalated O-atoms get drawn out from underneath the flakes, form water on the plain Ir patches and desorb. The other explanation is that OH and H_2O forms underneath the functionalized graphene flakes, but the dense phase is unstable and cannot be trapped and instead the molecules exit from underneath the graphene as soon as they are formed. Since both, the incomplete intercalation of hydrogen and the carbon clusters are indicated by a shoulder on the low BE side of the peak at 284.09 eV and the spectra were taken in snapshot mode, conclusions about the shape of the peaks should be drawn carefully. Hence, H-intercalation of the sample cannot be ruled out. Just like in panel a, the peak of the sample with carbon clusters remains at its higher energy position for 27 s during ever pulse and then changes back to indicate O-intercalation at 283.60 eV. The tails of these shifts from 284.09 eV to 283.60 eV are visibly longer than in the sample in panel a,

but comparable in shape. Since no intercalation is observable underneath the flakes with clusters, the effect can not be attributed to the OH and H_2O molecules but must originate from the O-atoms moving in underneath the flakes slower than the H-atoms.

In order to probe the kinetics of the system, the temperature was lowered to 45°C and the experiment was repeated. In panel a, without carbon clusters, the first pulse is misshapen, because the gas-dosing system malfunctioned and the sample was exposed to hydrogen for a too short time. Hence, we will focus on the three last pulses. It is interesting to note, that before the first pulse, the peak position is at 284.59 eV which is the oxygen intercalated position at 75°C, but after the pulse it only shifts back to 284.61 eV. That seems to be the peak position for O-intercalated graphene at 45°C. Upon arrival of the hydrogen pulses, the peak shifts from 284.62 eV to 283.33 eV within two frames or 1.4 s. The peak position of 284.33 eV is close to the value measured at 75°C and we again conclude that a dense OH-H_2O phase is intercalated under parts of the graphene flakes. The time, the water phase is intercalated changes slightly with increasing pulse count. It is 21 s, 22 s and 23 s for the last three pulses. The shift back to the O-intercalated peak position at 283.61 eV has a tail that is longer than even the functionalized sample at the higher temperature of 75°C takes for this shift. That means that the mobility of the O-atoms moving in underneath the sample is significantly reduced for this lower temperature.

The first pulse in panel (b) with the carbon clusters is too short, just like in panel a, and similarly to the unfunctionalized sample we can see the peak position indicating O-intercalation change from 283.60 eV before to 283.68 eV after the pulse. Again, the initial 283.60 eV and 283.68 eV represent the maximal O-intercalation at 75°C and 45°C, respectively. This 0.08 eV difference indicates that the surface-density of oxygen that manages to intercalate the graphene flakes with clusters at 45°C is smaller than for 75°C. Comparing panel (b) to panel (a) of figure 21 while relating to figure 19 which was recorded at 75°C, we observe that the shift from O-intercalation to higher binding energy takes 5 frames per pulse, corresponding to 3.5 s. That is about 2 s longer than both, the pulses in panel (a) of the same figure and the pulses with functionalized graphene at 75°C in figure 19. The higher binding energy in this case is 284.25 eV, which is a difference of -0.08 eV to the position of the graphene without clusters in panel a.

More significant it is the shift of +0.16 eV in comparison to the same sample at higher temperature. Whilst at 75°C no intercalation of the OH-H_2O phase was visible, now the peak is clearly shifted, indicating water being trapped underneath the graphene. This indicates that at 75°C, too, OH and H_2O have formed, but those molecules left right after formation and their residence time underneath the graphene flakes was too short

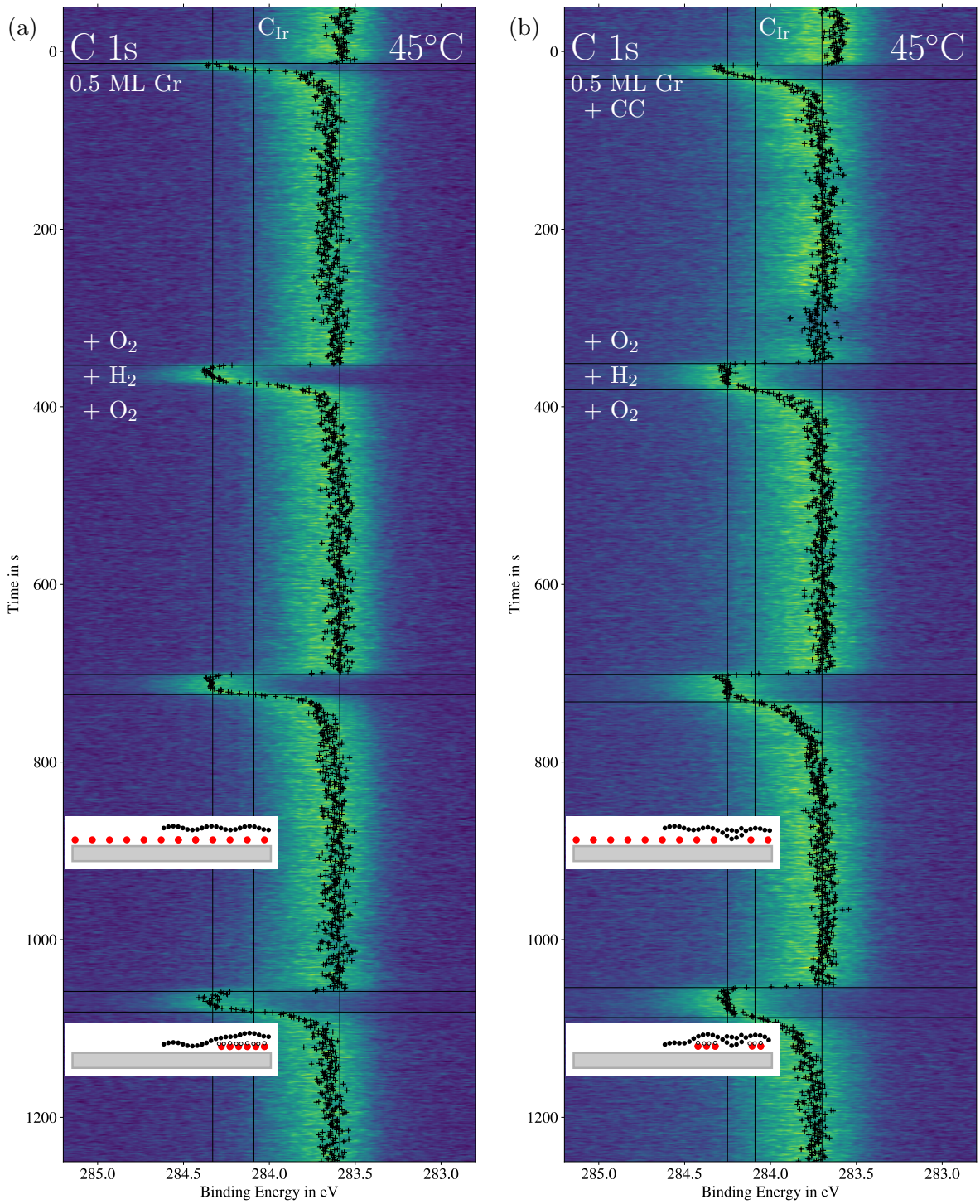

Figure 21: (a) Image plot with XP-spectra of 0.5 ML pristine graphene during exposure to O_2 while pulsing H_2 at 45°C. (b) Image plot with XP-spectra of C-functionalized graphene.

to observe. At 45°C the kinetic energy of these molecules has reduced, and they are no longer mobile enough to leave the flakes.

The durations of the pulses are 29 s, 31 s and 34 s. Those times are longer than any other

pulse times recorded.
The tail at the end of the pulses is much longer than during the other pulses which can be attributed to the combination of pinning down due to the clusters and the lower temperature, reducing the mobility of the O-atoms on their way in.

4 Conclusion

The highlights of this thesis are:
The C 1s fingerprint of 0.5 ML graphene flakes after exposure to atomic carbon contains the components that are characteristic for domelike C-clusters observed on 1.0 ML. These clusters induce diamond like sp^3-hybridization of individual C-atoms positioned at the perimeter of the C-clusters. As a result, the neighboring graphene bind downward to the iridium, and thereby pins the entire graphene flakes down, closer to the substrate.
Both, the pristine and the C-functionalized graphene, experience a decreased binding energy upon exposure to O_2. That signals lifting and decoupling of the graphene flakes from the Ir substrate. The binding energy of the C-functionalized graphene flakes decreases less as compared non-functionalized flakes. Further, a small component indicating sp^3-hybridization remains for functionalized flakes. The small sp^3-component implies that the number of C-atoms binding directly down to the Ir(111)-substrate has reduced, but they are still pinning the flakes closer to the substrate, marked by the lower binding energy compared to the sample without clusters.
Upon exposure to H_2 pulses at 75°C, a dense OH-H_2O phase is formed and trapped underneath the O-intercalated graphene flakes without C-clusters whereas no OH-H_2O phase is trapped below the functionalized graphene flakes. However, the same OH-H_2O phase, can be observed below both pristine and C-functionalized graphene if the experiment is repeated at 45°C instead of 75°C. These observations suggest that the intercalated O also has formed water with the hydrogen at 75°C for C-functionalized flakes, but in this case the flakes de-intercalate, the water is pressed out and no OH-H_2O phase is trapped. That means that the OH-H_2O phase is unstable underneath the C-functionalized graphene flakes.

5 Outlook

While many effects of C-functionalization on top of graphene flakes on water formation below have been mapped out, some questions remain unanswered and new ones have emerged.

During O-intercalation, though a reduction of sp^3-hybridized atoms is observed, it remains unclear, how the structure of the C-clusters atop the graphene flakes is affected by the intercalation. DFT calculations could, for example, shed light on that. Furthermore, in order to examine whether these changes are permanent, the graphene flakes should be characterized after deintercalation of the oxygen by annealing. The same should be done after intercalation of the OH-H_2O phase.
STM images of the C-functionalized graphene flakes during intercalation of the OH-H_2O phase can determine the positions of the intercalated pieces of the flakes related to the positions of the clusters.
Most interesting would be to observe the O 1s region of both, pristine and C-functionalized graphene during intercalation of the OH-H_2O phase and compare the ratios between the OH and H_2O concentrations underneath the flakes. This different ratio would demonstrate the capability of the C-clusters to modify the selectivity underneath the graphene. That would be a crucial change of the catalytic properties of the graphene flakes and pave the way for investigation of similar effects in other, more complex reactions with different reaction paths.

References

[1] Elin Grånäs et al. "Water chemistry beneath graphene: formation and trapping of a super-dense OH-H2O phase". In: *not yet published* ().

[2] K. S. Novoselov et al. "Electric Field Effect in Atomically Thin Carbon Films". In: *Science* 306.5696 (2004), pp. 666–669. ISSN: 0036-8075. DOI: 10.1126/science.1102896. eprint: https://science.sciencemag.org/content/306/5696/666.full.pdf. URL: https://science.sciencemag.org/content/306/5696/666.

[3] Alpha T N'Diaye et al. "Structure of epitaxial graphene on Ir(111)". In: *New Journal of Physics* 10.4 (Apr. 2008), p. 043033. DOI: 10.1088/1367-2630/10/4/043033. URL: https://doi.org/10.1088%2F1367-2630%2F10%2F4%2F043033.

[4] Elin Grånäs et al. "Hydrogen intercalation under graphene on Ir(111)". In: *Surface Science* 651 (2016), pp. 57–61. ISSN: 0039-6028. DOI: https://doi.org/10.1016/j.susc.2016.03.002. URL: http://www.sciencedirect.com/science/article/pii/S0039602816000996.

[5] C. Riedl et al. "Quasi-Free-Standing Epitaxial Graphene on SiC Obtained by Hydrogen Intercalation". In: *Phys. Rev. Lett.* 103 (24 Dec. 2009), p. 246804. DOI:

10.1103/PhysRevLett.103.246804. URL: https://link.aps.org/doi/10.1103/PhysRevLett.103.246804.

[6] Rosanna Larciprete et al. "Oxygen Switching of the Epitaxial Graphene–Metal Interaction". In: *ACS Nano* 6.11 (2012). PMID: 23051045, pp. 9551–9558. DOI: 10.1021/nn302729j. eprint: https://doi.org/10.1021/nn302729j. URL: https://doi.org/10.1021/nn302729j.

[7] Elin Grånäs et al. "Oxygen Intercalation under Graphene on Ir(111): Energetics, Kinetics, and the Role of Graphene Edges". In: *ACS Nano* 6.11 (2012). PMID: 23039853, pp. 9951–9963. DOI: 10.1021/nn303548z. eprint: https://doi.org/10.1021/nn303548z. URL: https://doi.org/10.1021/nn303548z.

[8] Elin Grånäs et al. "CO Intercalation of Graphene on Ir(111) in the Millibar Regime". In: *The Journal of Physical Chemistry C* 117.32 (2013), pp. 16438–16447. DOI: 10.1021/jp4043045. eprint: https://doi.org/10.1021/jp4043045. URL: https://doi.org/10.1021/jp4043045.

[9] Rentao Mu et al. "Visualizing Chemical Reactions Confined under Graphene". In: *Angewandte Chemie International Edition* 51.20 (2012), pp. 4856–4859. DOI: 10.1002/anie.201200413. eprint: https://onlinelibrary.wiley.com/doi/pdf/10.1002/anie.201200413. URL: https://onlinelibrary.wiley.com/doi/abs/10.1002/anie.201200413.

[10] Yanhong Zhang et al. "Enhanced reactivity of graphene wrinkles and their function as nanosized gas inlets for reactions under graphene". In: *Phys. Chem. Chem. Phys.* 15 (43 2013), pp. 19042–19048. DOI: 10.1039/C3CP52115J. URL: http://dx.doi.org/10.1039/C3CP52115J.

[11] Elin Grånäs. *Above and below graphene: nanoparticle chemistry and interface reactions*. Lund University, 2014.

[12] Charlotte Herbig et al. "From Permeation to Cluster Arrays: Graphene on Ir(111) Exposed to Carbon Vapor". In: *Nano Letters* 17.5 (2017). PMID: 28426934, pp. 3105–3112. DOI: 10.1021/acs.nanolett.7b00550. eprint: https://doi.org/10.1021/acs.nanolett.7b00550. URL: https://doi.org/10.1021/acs.nanolett.7b00550.

[13] Richard Balog et al. "Atomic Hydrogen Adsorbate Structures on Graphene". In: *Journal of the American Chemical Society* 131.25 (2009). PMID: 19496562, pp. 8744–8745. DOI: 10.1021/ja902714h. eprint: https://doi.org/10.1021/ja902714h. URL: https://doi.org/10.1021/ja902714h.

[14] M. L. Ng et al. “Controlling Hydrogenation of Graphene on Transition Metals”. In: *The Journal of Physical Chemistry C* 114.43 (2010), pp. 18559–18565. DOI: 10.1021/jp106361y. eprint: https://doi.org/10.1021/jp106361y. URL: https://doi.org/10.1021/jp106361y.

[15] Richard Balog et al. “Controlling Hydrogenation of Graphene on Ir(111)”. In: *ACS Nano* 7.5 (2013). PMID: 23586740, pp. 3823–3832. DOI: 10.1021/nn400780x. eprint: https://doi.org/10.1021/nn400780x. URL: https://doi.org/10.1021/nn400780x.

[16] María Escudero-Escribano. “Electrocatalysis and surface nanostructuring : atomic ensemble effects and non-covalent interactions”. PhD thesis. Nov. 2011.

[17] P. D. Zavitsanos and G. A. Carlson. “Experimental study of the sublimation of graphite at high temperatures”. In: *The Journal of Chemical Physics* 59.6 (1973), pp. 2966–2973. DOI: 10.1063/1.1680430. eprint: https://doi.org/10.1063/1.1680430. URL: https://doi.org/10.1063/1.1680430.

[18] Johann Coraux et al. “Growth of graphene on Ir (111)”. In: *New Journal of Physics* 11.2 (2009), p. 023006.

[19] David R Linde. *CRC handbook of chemistry and physics*. Vol. 90. 1993, p. 1981.

[20] Jan Knudsen et al. “Clusters binding to the graphene moiré on Ir(111): X-ray photoemission compared to density functional calculations”. In: *Phys. Rev. B* 85 (3 Jan. 2012), p. 035407. DOI: 10.1103/PhysRevB.85.035407. URL: https://link.aps.org/doi/10.1103/PhysRevB.85.035407.

[21] Timm Gerber et al. “CO-Induced Smoluchowski Ripening of Pt Cluster Arrays on the Graphene/Ir(111) Moiré”. In: *ACS Nano* 7.3 (2013). PMID: 23379255, pp. 2020–2031. DOI: 10.1021/nn400082w. eprint: https://doi.org/10.1021/nn400082w. URL: https://doi.org/10.1021/nn400082w.

[22] N. A. Vinogradov et al. “Impact of Atomic Oxygen on the Structure of Graphene Formed on Ir(111) and Pt(111)”. In: *The Journal of Physical Chemistry C* 115.19 (2011), pp. 9568–9577. DOI: 10.1021/jp111962k. eprint: https://doi.org/10.1021/jp111962k. URL: https://doi.org/10.1021/jp111962k.